Radical Polymerization of Styrene Controlled by Half-Sandwich Mo(III)/Mo(IV) Couples: All Basic Mechanisms Are Possible

Erwan Le Grognec,[†] Jérôme Claverie,*[,‡] and Rinaldo Poli*[,†]

Contribution from the Laboratoire de Synthèse et d'Electrosynthèse Organométalliques, Faculté des Sciences "Gabriel", Université de Bourgogne, 6 Boulevard Gabriel, 21000 Dijon, France, and the Laboratoire de Chimie des Procédés de Polymérisation, LCPP/CPE-CNRS 43, Boulevard du 11 Novembre 1918, 69616 Villeurbanne, France

Received April 19, 2001

Abstract: Density functional calculations of bond dissociation energies (BDEs) have been used as a guide to the choice of metal system suitable for controlling styrene polymerization by either the stable free radical polymerization (SFRP) or the atom transfer radical polymerization (ATRP) mechanism. In accord with the theoretical prediction, CpMo(η^4-C_4H_6)(CH_2SiMe_3)$_2$, **2**, is not capable of yielding SFRP of styrene. Still in accord with theoretical prediction, CpMo(η^4-C_4H_6)Cl_2, **1**, CpMo(PMe_3)$_2Cl_2$, **3**, and CpMo(dppe)Cl_2 (dppe = 1,2-bis(diphenylphosphino)ethane), **4**, yield controlled styrene polymerization by the SFRP mechanism in the presence of 2,2′-azobisisobutyronitrile (AIBN). This arises from the generation of a putative Mo(IV) alkyl species from the AIBN-generated radical addition to the Mo(III) compound. The controlled nature of the polymerizations is indicated by linear M_n progression with the conversion in all cases and moderate polydispersity indices (PDIs). Controlled polymerization of styrene is also given by compounds **3** and **4** in combination with alkyl bromides. These complexes then operate by the ATRP mechanism, again in accord with the theoretical predictions. Controlled character is revealed by linear increase of M_n versus conversion, low PDIs, a stop-and-go experiment, and ^{1}H NMR and MALDI-TOF analyses of the polymer end groups. The same controlled polymerization is given by a "reverse" ATRP experiment, starting from AIBN and CpMo(PMe_3)$_2Cl_2$Br, **5**. On the other hand, when compound **1** or **2** is used in combination with an alkyl bromide (as for an ATRP experiment), the isolated polystyrene shows by M_n, ^{1}H NMR, and MALDI-TOF analyses that catalytic chain transfer (CCT) radical polymerization takes place in this case. Kinetics simulations underscore the conditions regulating the radical polymerization mechanism and the living character of the polymerization. The complexes herein described are ineffective at controlling the polymerization of methyl methacrylate.

Introduction

The development of well-defined macromolecular architectures by controlled polymerization techniques has appeared to be the goal of numerous academic as well as industrial laboratories.[1] The field of "living" polymerization has drastically changed with the appearance of controlled/"living" radical polymerization, because radical polymerization is generally more tolerant to polar functionalities than are anionic, cationic, and coordination polymerizations. Although there were less than 20 relevant reports in 1993, more than 800 papers and patents have dealt with the subject in 1999.[2,3] With the exception of reversible addition fragmentation transfer (RAFT) polymerization,[4] control of radical polymerization is exerted through the interaction of a free radical (the active species during the polymerization) and a spin trap that can be organic or inorganic in nature. The fundamental concept that is underlying the majority of these polymerizations is the persistent radical effect (PRE).[5,6]

Scheme 1

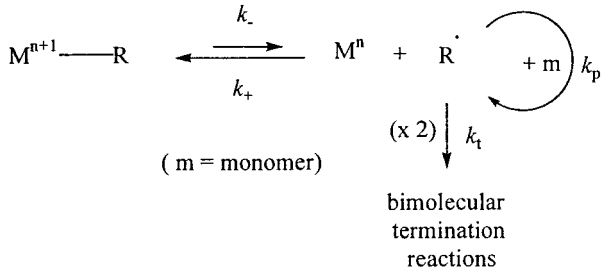

In stable free radical polymerization (SFRP), a fast reversible equilibrium is established between an SFR (or persistent radical) and a reactive free radical on one side and a dormant species on the other side (see Scheme 1). Bimolecular terminations by radical−radical coupling or disproportionation result in an increase of the [SFR]:[free radicals] ratio, thus biasing the reaction manifold toward SFR and free radical cross-coupling. As a result, bimolecular radical termination reactions are virtually suppressed and the polymerization becomes controlled, as shown by narrow molecular weight distributions (polydis-

* To whom correspondence should be addressed. Phone: +33-3-80-39-68-81. Fax: +33-3-80-39-60-98. E-mail: Rinaldo.Poli@u-bourgogne.fr.
† Université de Bourgogne.
‡ Laboratoire de Chimie des Procédés de Polymérisation.

(1) Yeates, S. G.; Richards, S. N. *Surf. Coat. Int.* **1996**, *1996*, 437−441.
(2) Matyjaszewski, K. *Controlled Radical Polymerization*; American Chemical Society: Washington, DC, 1998.
(3) Patten, T. E.; Matyjaszewski, K. *Acc. Chem. Res.* **1999**, *32*, 895−903.
(4) Chiefari, J.; Chong, Y. K.; Ercole, F.; Krstina, J.; Jeffery, J.; Le, T. P. T.; Mayadunne, R. T. A.; Meijs, G. F.; Moad, C. L.; Moad, G.; Rizzardo, E.; Thang, S. H. *Macromolecules* **1998**, *31*, 5559−5562.
(5) Fischer, H. *J. Am. Chem. Soc.* **1986**, *108*, 3925−3927.
(6) Fischer, H. *Macromolecules* **1997**, *30*, 5666−5672.

10.1021/ja010998d CCC: $20.00
Published on Web 09/11/2001

Scheme 2

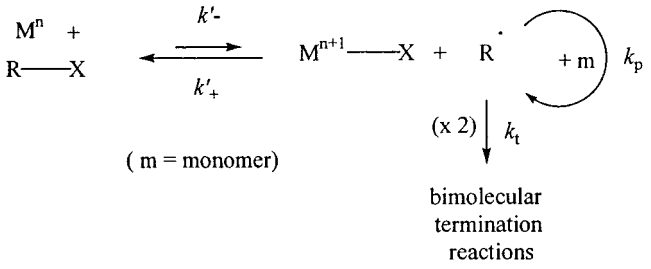

persity index, PDI, as low as 1.05), a number average molecular weight that linearly increases with conversion, apparent first-order kinetics, and the possibility to synthesize well-defined macromolecules with complex architectures (block, comb, start, dendritic, hyperbranched, etc.).[7,8]

The concept of SFRP, first developed for organic nitroxide SFR,[9,10] was generalized to other organic species[11,12] and to transition metal SFR, such as cobalt[13,14] and iron species.[15] However, the most successful implementation of the PRE has been through the intervention of an atom transfer mechanism. In atom transfer radical polymerization (ATRP), a halogen capped dormant chain and a metal complex are in fast equilibrium with a polymeric free radical and a metal halide complex, the latter playing the role of spin trap (see Scheme 2).

Although many different systems based on Fe(II),[16−19] Ni(II),[20−22] Ru(II),[23−26] Re(V),[27] Mo(V),[28] Pd(0),[29] Co(II),[30] and Rh(I)[31,32] exist, the most utilized systems are Cu(I) based systems, first developed by Matyjaszewski.[8,33]

Scheme 3

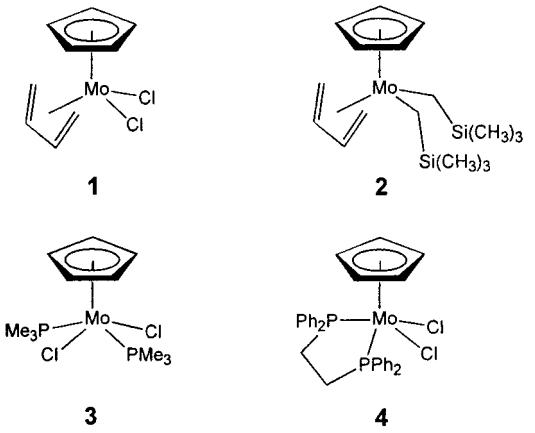

When dealing with the organometallic PRE,[34] a major difference between SFRP and ATRP lies in the fact that the reactivity is dictated by the strength of the metal−alkyl bond in the former case and by the strengths of the metal−halide and alkyl−halide bonds in the latter one. Albeit numerous SFRP and ATRP promoters are known as mentioned above, there are, to our knowledge, no detailed studies of the selecting rules allowing the prediction of the behavior of a given organometallic compound as a controller in radical polymerization. Rather, many promoters are now discovered through the use of high throughput techniques, which would benefit from mechanistic studies.[35−37] Our knowledge of half-sandwich molybdenum complexes[38] in terms of structural parameters and of radical reactivity has prompted us to use them as model compounds in SFRP and in ATRP. Through the use of these complexes, we endeavor to generate preliminary mechanistic arguments in order to contribute to the comprehension of the mechanism of free radical polymerization controlled by an organometallic compound.

In this paper, we first present theoretical results that guide us toward the choice of half-sandwich Mo(III) systems in these polymerizations. After describing the Mo(III) and Mo(IV) complexes used in this work (see Scheme 3), we illustrate their application in styrene radical polymerization. The results reported here show how, in agreement with theoretical predictions, the same family of compounds can control radical polymerization by both SFRP and ATRP mechanisms. Furthermore, it will be shown that a slight change in ligand substitution pattern directs the reaction to totally different manifolds, namely living polymerization versus catalytic chain transfer (CCT, see Scheme 4)[39−43] polymerization. This behavior can be rational-

(7) Hawker, C. J. *Acc. Chem. Res.* **1997**, *30*, 373−382 and reference therein.
(8) Coessens, V.; Pintauer, T.; Matyjaszewski, K. *Prog. Polym. Sci.* **2001**, *26*, 337−377 and reference therein.
(9) Solomon, D. H.; Rizzardo, E.; Cacioli, P. Eur. Pat. 135280, 1985; *Chem. Abs.* **1985**, *85*, P25381t.
(10) Rizzardo, E. *Chem. Aust.* **1987**, *54*, 32−43.
(11) Otsu, T.; Tazaki, T. *Polym. Bull.* **1986**, *16*, 277−284.
(12) Colombani, D.; Steenbock, M.; Klapper, M.; Müllen, K. *Macromol. Rapid. Commun.* **1997**, *18*, 243−251.
(13) Arvanatitopoulos, L. D.; Greuel, M. P.; Harwood, H. J. *Polym. Prepr. (Am. Chem. Soc., Div. Polym. Chem.)* **1994**, *34*, 549−551.
(14) Wayland, B.; Poszmick, G.; Mukerjee, S. *J. Am. Chem. Soc.* **1994**, *116*, 7943−7944.
(15) Claverie, J. *Res. Discl.* **1998**, *416*, 1595−1604.
(16) Matyjaszewski, K.; Wei, M.; Xia, J.; McDermott, N. E. *Macromolecules* **1997**, *30*, 8161−8164.
(17) Ando, T.; Kamigaito, M.; Sawamoto, M. *Macromolecules* **1997**, *30*, 4507−4510.
(18) Kotani, Y.; Kamigaito, M.; Sawamoto, M. *Macromolecules* **2000**, *33*, 3543−3549.
(19) Louie, J.; Grubbs, R. H. *Chem. Commun.*, not yet published.
(20) Granel, C.; Dubois, P.; Jerome, R.; Teyssie, P. *Macromolecules* **1996**, *29*, 8576−8582.
(21) Uegaki, H.; Kotani, Y.; Kamigaito, M.; Sawamoto, M. *Macromolecules* **1997**, *30*, 2249−2253.
(22) Uegaki, H.; Kotani, Y.; Kamigaito, M.; Sawamoto, M. *Macromolecules* **1998**, *31*, 6756−6761.
(23) Simal, S.; Demonceau, A.; Noels, A. F. *Angew. Chem., Int. Ed.* **1999**, *38*, 538−540.
(24) Simal, F.; Demonceau, A.; Noels, A. F. *Tetrahedron Lett.* **1999**, *40*, 5689−5693.
(25) del Rio, I.; van Koten, G.; Lutz, M.; Spek, A. L. *Organometallics* **2000**, *19*, 361−364.
(26) Kato, M.; Kamigaito, M.; Sawamoto, M.; Higashimura, T. *Macromolecules* **1995**, *28*, 1721−1723.
(27) Kotani, Y.; Kamigaito, M.; Sawamoto, M. *Macromolecules* **1999**, *32*, 2420−2424.
(28) Brandts, J. A. M.; van de Geijn, P.; van Faassen, E. E.; Boersma, J.; van Koten, G. *J. Organomet. Chem.* **1999**, *584*, 246−253.
(29) Lecomte, P.; Draiper, I.; Dubois, P.; Teyssié, P.; Jérôme, R. *Macromolecules* **1997**, *30*, 7631−7633.
(30) Christie, D.; Claverie, J.; Kanagasabapathy, S. WO 0059954 A, 1999.
(31) Moineau, C.; Minet, M.; Teyssié, P.; Jérôme, R. *Macromolecules* **1999**, *32*, 8277−8282.
(32) Percec, V.; Barboiu, B.; Neumann, A.; Ronda, J. C.; Zhao, M. *Macromolecules* **1996**, *29*, 3665−3668.
(33) Wang, J.-S.; Matyjaszewski, K. *J. Am. Chem. Soc.* **1995**, *117*, 5614−5615.
(34) It is to be noted that the usage of SFR and PRE is inappropriate when the spin trap does not have radical character.
(35) Huefner, P.; Jandeleit, B.; Klaerner, G.; Yunxiao, L.; Nielsen, B. R.; Safir, A. WO 0053640, 2000.
(36) Benoit, D.; Chaplinski, V.; Braslau, R.; Hawker, C. J. *J. Am. Chem. Soc.* **1999**, *121*, 3904−3920.
(37) Hodges, J. C.; Harikrishnan, L. S.; Ault-Justus, S. *J. Comb. Chem.* **2000**, *2*, 80−88.
(38) Poli, R. *J. Coord. Chem.* **1993**, *29*, 121−173.
(39) Heuts, J. P. A.; Forster, D. J.; Davis, T. P.; Yamada, B.; Yamazoe, H.; Azukizawa, M. *Macromolecules* **1999**, *32*, 2511−2519.
(40) Enikolopyan, N. S.; Smirnov, B. R.; Ponomarev, G. V.; Belgovskii, I. M. *J. Polym. Sci., Polym. Chem. Ed.* **1981**, *19*, 879−889.
(41) Kukulj, D.; Heuts, J. P.; Davis, T. P. *Macromolecules* **1998**, *31*, 6034−6041.

Scheme 4

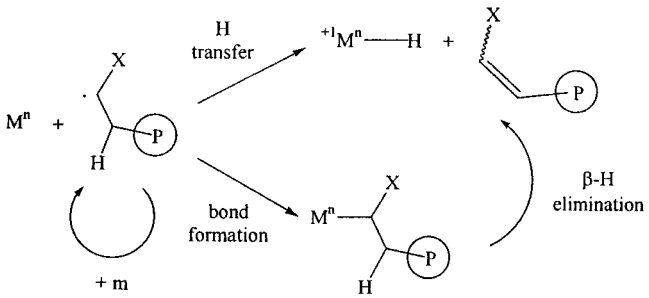

ized on the basis of a global kinetic model. Although the reversible bond formation in CCT and in SFRP is well-known,[39] the fact that the same complex is active in both processes under slightly different conditions is unprecedented.

Results and Discussion

A. Theoretical Studies. The homolytic bond dissociation energy (BDE) of the Mo−X bond in half-sandwich Mo(II) compounds has already been investigated and recently reported by some of us.[44] The system under study was $CpMoX(PH_3)_3$ (X = H, CH_3, F, Cl, Br, I, OH, PH_2). In particular, the BDE values for the bonds with Cl, Br, and CH_3, of relevance to our present study, were found to be 73.1, 63.1, and 40.5 kcal/mol, respectively. These BDEs are so high that these complexes are not expected to have activity in SFRP or ATRP (vide infra).

We have then carried out BDE investigations of the Mo−X bond for the half-sandwich Mo(III) systems $CpMoX_2L_2$, with X = Cl and CH_3 and with L = PH_3 and PMe_3, or L_2 = η^4-C_4H_6, for which examples are experimentally available from this and other laboratories.[45−55] The BDEs have been calculated by subtracting the energy of the geometry-optimized 17-electron system $CpMoX_2L_2$ from the sum of the energies of the two separated and geometry-optimized $CpMoXL_2$ and X fragments (eq 1). The calculations were carried out at the B3LYP/LANL2DZ level, which has proven satisfactory for the type of systems investigated here, affording results within < 5 kcal/mol of the experiment.[56−58]

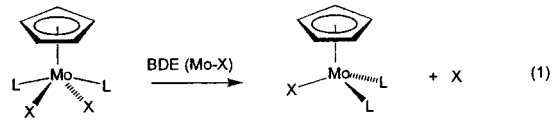

All relevant energetic results are collected in Table 1, while selected optimized geometric parameters are listed in Table 2.

Table 1. Relevant Energetic Parameters for Geometry-Optimized $CpMoX_2L_2$/$CpMoXL_2$ + X Systems

L	X	BDE (kcal/mol)[a]	E_{S-T} (kcal/mol)[b]
PH_3	Cl	69.2	7.5
η^4-C_4H_6	Cl	60.4	4.1
PH_3	CH_3	36.5	3.1
PMe_3	CH_3	37.2	7.5
η^4-C_4H_6	CH_3	38.5	7.3

[a] BDE = $E(CpMoX_2L_2) - E(CpMoXL_2) - E(X)$. The 16-electron $CpMoXL_2$ complex is optimized in the triplet state. [b] $E_{S-T} = E$(singlet)-E(triplet) for $CpMoXL_2$.

Table 2. Selected Optimized Geometric Parameters for Doublet $CpMoX_2L_2$ and Triplet $CpMoXL_2$[a]

	Mo−Cp(CNT) (Å)	Mo−X (Å)	Mo−L (Å)
$CpMoCl_2(PH_3)_2$	2.075	2.534	2.544
$CpMoCl(PH_3)_2$	2.041	2.472	2.538
$CpMo(CH_3)_2(PH_3)_2$	2.052	2.259	2.530
$CpMo(CH_3)(PH_3)_2$	2.099	2.193	2.515
$CpMo(CH_3)_2(PMe_3)_2$	2.056	2.266	2.571
$CpMo(CH_3)(PMe_3)_2$	2.117	2.199	2.530
$CpMoCl_2(\eta^4$-$C_4H_6)$	2.066	2.501	2.051,[b] 2.273[c]
$CpMoCl(\eta^4$-$C_4H_6)$	2.107	2.482	2.272,[b] 2.313[c]
$CpMo(CH_3)_2(\eta^4$-$C_4H_6)$	2.123	2.225	2.286,[b] 2.362[c]
$CpMo(CH_3)(\eta^4$-$C_4H_6)$	2.151	2.191	2.262,[b] 2.317[c]
$CpMoCl_2$(dpe)	2.019	2.532	2.533
CpMoCl(dpe)	2.046	2.491	2.519
$CpMo(CH_3)_2$(dpe)	2.044	2.236	2.509
$CpMo(CH_3)$(dpe)	2.110	2.196	2.500

[a] Chemically equivalent distances are averaged. [b] Bond between Mo and external carbon. [c] Bond between Mo and internal carbon.

The geometry-optimized $CpMoX(PH_3)_2$ (X = Cl, CH_3) and $CpMoCl_2(PH_3)_2$ systems were already available as part of previous studies.[44,59] Calculations on $CpMoCl_2(PH_3)_2$ have also been previously published, although at a slightly different level of theory.[60,61] As previously found for $CpMoX(PH_3)_2$, the 16-electron $CpMoX(PMe_3)_2$ and $CpMoX(\eta^4$-$C_4H_6)$ systems are calculated to have a ground state triplet configuration [experimentally verified for $Cp^*MoCl(PMe_3)_2$];[62,63] thus, the BDE values are given relative to this configuration. The optimized geometries of $CpMoCl_2(\eta^4$-$C_4H_6)$ and $CpMo(CH_3)_2(\eta^4$-$C_4H_6)$ are quite close to the experimentally established ones.[48,54] Because of warnings about the use of PH_3 as a model for trialkylphosphines,[64,65] we have carried out calculations on the bisphosphine dimethyl system by using also the "real" PMe_3 system, all atoms being treated quantum mechanically. The results in terms of both energies (Table 1) and geometries (Table 2) are quite comparable with those obtained with the simpler

(42) Gridnev, A. A.; Ittel, S. D.; Wayland, B. B.; Fryd, M. *Organometallics* **1996**, *15*, 5116−5126.
(43) Burczyk, A. F.; O'Driscoll, F.; Rempel, G. L. *J. Polym. Sci., Polym. Chem. Ed.* **1984**, *22*, 3255−3262.
(44) Cacelli, I.; Poli, R.; Quadrelli, E. A.; Rizzo, A.; Smith, K. M. *Inorg. Chem.* **2000**, *39*, 517−524.
(45) Poli, R. *Synlett* **1999**, 1019−1028.
(46) Poli, R.; Krueger, S. T.; Abugideiri, F.; Haggerty, B. S.; Rheingold, A. L. *Organometallics* **1991**, *10*, 3041−3046.
(47) Davidson, J. L.; Davidson, K.; Lindsell, W. E. *J. Chem. Soc., Chem. Commun.* **1983**, 452−453.
(48) Davidson, J. L.; Davidson, K.; Lindsell, W. E.; Murrall, N. W.; Welch, A. J. *J. Chem. Soc., Dalton Trans.* **1986**, 1677−1688.
(49) Wang, L.-S.; Fettinger, J. C.; Poli, R. *J. Am. Chem. Soc.* **1997**, *119*, 4453−4464.
(50) Poli, R.; Wang, L.-S. *J. Am. Chem. Soc.* **1998**, *120*, 2831−2842.
(51) Wang, L.-S.; Fettinger, J. C.; Poli, R.; Meunier-Prest, R. *Organometallics* **1998**, *17*, 2692−2701.
(52) Poli, R.; Wang, L.-S. *Coord. Chem. Rev.* **1998**, *178−179*, 169−189.
(53) Le Grognec, E.; Poli, R.; Wang, L.-S. *Inorg. Chem. Commun.* **1999**, *2*, 95−96.
(54) Le Grognec, E.; Poli, R.; Richard, P. *Organometallics* **2000**, *19*, 3842−3853.
(55) Le Grognec, E.; Poli, R.; Richard, P. *J. Chem. Soc., Dalton Trans.*, in press.
(56) Keogh, D. W.; Poli, R. *J. Chem. Soc., Dalton Trans.* **1997**, 3325−3333.
(57) Poli, R.; Smith, K. M. *Organometallics* **2000**, *19*, 2858−2867.
(58) Smith, K. M.; Poli, R.; Harvey, J. N. *Chem.—Eur. J.* **2001**, *7*, 1679−1690.
(59) Smith, K. M.; Poli, R.; Harvey, J. N. *New J. Chem.* **2000**, *24*, 77−80.
(60) Cacelli, I.; Keogh, D. W.; Poli, R.; Rizzo, A. *New J. Chem.* **1997**, *21*, 133−135.
(61) Cacelli, I.; Keogh, D. W.; Poli, R.; Rizzo, A. *J. Phys. Chem. A* **1997**, *101*, 9801−9812.
(62) Abugideiri, F.; Keogh, D. W.; Poli, R. *J. Chem. Soc., Chem. Commun.* **1994**, 2317−2318.
(63) Abugideiri, F.; Fettinger, J. C.; Keogh, D. W.; Poli, R. *Organometallics* **1996**, *15*, 4407−4416.
(64) Jacobsen, H.; Berke, H. *Chem.—Eur. J.* **1997**, *3*, 881−886.
(65) Schmid, R.; Herrmann, W. A.; Frenking, G. *Organometallics* **1997**, *16*, 701−708.

Table 3. Selected Optimized Geometric Parameters for $CpMoCl_2X(PH_3)_n$ ($n = 2, 1$)

X	*n*	Mo−Cp(CNT) (Å)	Mo−X (Å)	Mo−Cl_{eq} (Å)[a]	Mo−PH_3 (Å)[a]
Cl	2	2.039	2.563	2.582	2.554
Br	2	2.038	2.773	2.579	2.554
CH_3	2	2.057	2.279	2.602	2.543
Br	1[b]	2.087	2.585	2.493	2.604

[a] Chemically equivalent distances are averaged. [b] Calculated in the triplet state.

PH_3 model. Therefore, all other calculations on phosphine containing molecules reported in this contribution have been carried out using the PH_3 model.

It can be remarked from Table 1 that the Mo−X BDE changes only by a very small amount by a change of ancillary ligand from PH_3 (or PMe_3) to C_4H_6. It may also be observed that the BDEs for the Mo(III)−X bonds are smaller than the corresponding Mo(II)−X BDEs mentioned above. The Mo(III)−CH_3 bond strengths are similar to those found in alkoxyamines, such as 2,2,5,5-tetramethyl-1-(-phenylethyloxy)piperidine, which are efficient in SFRP only above 125 °C (E_{dec} for TEMPO−CH(Ph)−CH_3 = 37 kcal/mol).[66,67] The Mo(III)−alkyl complexes are not sufficiently stable in order to carry out the polymerization under those conditions.[46,54]

The observed trend of BDEs on going from Mo(II) to Mo(III) made us predict a further decrease for Mo(IV) systems. We have, therefore, carried out additional calculations by focusing on the 18-electron $CpMoX_3L_2$ system, examples of which are available with L = phosphine ligand.[63,68−74] We have restricted our BDE calculations to the Mo−X bond in $CpMoCl_2X(PH_3)_2$, for X = Cl, Br, and CH_3, see eq 2. This restriction is

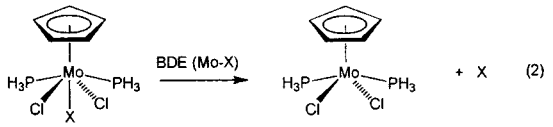

BDE (Mo-X) = 44.0 (Cl), 31.7 (Br), 24.3 (CH_3) (kcal/mol)

justified by the fact that the only experimentally available 18-electron $CpMo^{IV}$ systems are the trichlorides. Of the various possible isomers for the starting compound, we have considered those having the X ligand in a pseudoaxial position, that is, trans relative to the Cp ligand. The calculated BDE values are shown in eq 2, and the relevant geometric parameters of the optimized $CpMoCl_2X(PH_3)_2$ molecules are shown in Table 3. There is a very close correspondence between the calculated geometric parameters for $CpMoCl_3(PH_3)_2$ and those experimentally determined for $CpMoCl_3(PMe_2Ph)_2$.[63] For the specific example of $CpMoCl_2Br(PH_3)_2$, the corresponding isomer with axial Cl and equatorial Br gave an analogous BDE(Mo−Br) of 33.3 kcal/mol. The energetic results of the calculations confirm

Scheme 5

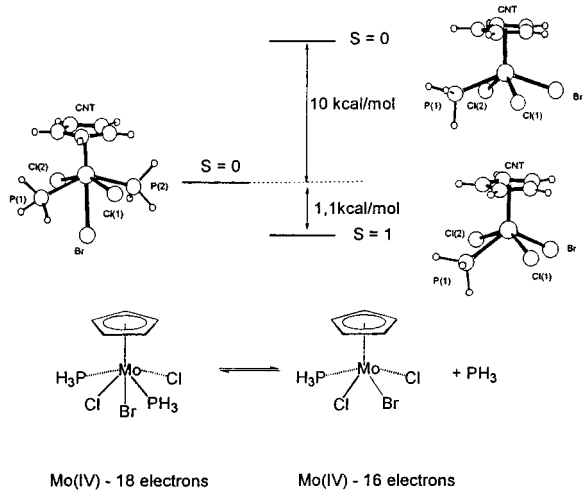

the expected decrease of BDE as the metal oxidation state increases from II to IV. The Mo−CH_3 BDE in the Mo(IV) compound examined falls in an interesting range for controlled radical polymerization at a temperature of 80 °C or below.[36,75]

The $CpMoCl_2Br(PH_3)_2$ system has also been examined with respect to the phosphine ligand dissociation process. The results are shown in Scheme 5. As experimentally verified for a few trichloride analogues,[63] the 16-electron Mo(IV) system has a spin triplet ground state. The low ΔE (1.1 kcal) value for the phosphine dissociation process involving the triplet product points to a probable equilibrium between the two species. The optimized geometry of triplet $CpMoCl_2Br(PH_3)$ is also included in Scheme 5 and is quite similar to that experimentally established for Cp^*MoCl_3L (L = PMe_3, $PMePh_2$).[63]

Final computational studies of relevance to this work are those shown in eqs 3 and 4. These correspond to the initiation

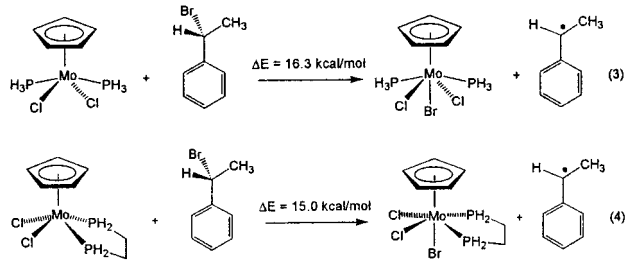

processes for a controlled radical polymerization by atom transfer.[76] The (1-bromoethyl)benzene initiator is the commonly used one for the radical polymerization of styrene and has also been used in this work. The only difference between the model reactions and the actual experimental systems is the use of the model phosphines PH_3 and $PH_2CH_2CH_2PH_2$ in place of PMe_3 and dppe, respectively. The calculated energies for these processes (16.3 and 15.0 kcal/mol) are rather accessible under thermal conditions and lead to the prediction that half-sandwich Mo(III)/Mo(IV) systems may be able to control a radical polymerization by the atom transfer mechanism.

B. Synthesis of Mo(IV) Complexes. The Mo(IV) complex $CpMo(PMe_3)_2Cl_2Br$, **5**, has been synthesized in order to evaluate the possibility of controlling a radical polymerization with the Mo(III)/Mo(IV) couple by the reverse ATRP methodology (vide

(66) Fukuda, T.; Terauchi, T.; Goto, A.; Ohno, K.; Tsujii, Y.; Miyamoto, T.; Kobatake, S.; Yamada, B. *Macromolecules* **1996**, *29*, 6393−6398.
(67) Fukuda, T.; Tsujii, Y.; Miyamoto, T. *Polym. Prepr. (Am. Chem. Soc., Div. Polym. Chem.)* **1997**, *38*, 723−725.
(68) Stärker, K.; Curtis, M. D. *Inorg. Chem.* **1985**, *24*, 3006−3010.
(69) Green, M. L. H.; Lindsell, W. E. *J. Chem. Soc. A* **1967**, 686−687.
(70) Aviles, T.; Green, M. L. H.; Dias, A. R.; Romão, C. *J. Chem. Soc., Dalton Trans.* **1979**, 1367−1371.
(71) Adams, G. S. B.; Green, M. L. H. *J. Chem. Soc., Dalton Trans.* **1981**, 353−356.
(72) Krueger, S. T.; Owens, B. E.; Poli, R. *Inorg. Chem.* **1990**, *29*, 2001−2006.
(73) Owens, B. E.; Poli, R. *Inorg. Chim. Acta* **1991**, *179*, 229−237.
(74) Poli, R.; Owens, B. E.; Linck, R. G. *J. Am. Chem. Soc.* **1992**, *114*, 1302−1307.
(75) Benoit, D.; Grimaldi, S.; Robin, S.; Finet, J. P.; Tordo, P.; Gnanou, Y. *J. Am. Chem. Soc.* **2000**, *122*, 5929−5939.
(76) Matyjaszewski, K.; Gaynor, S.; Greszta, D.; Mardare, D.; Shigemoto, T. *Macromol. Symp.* **1995**, *98*, 73−89.

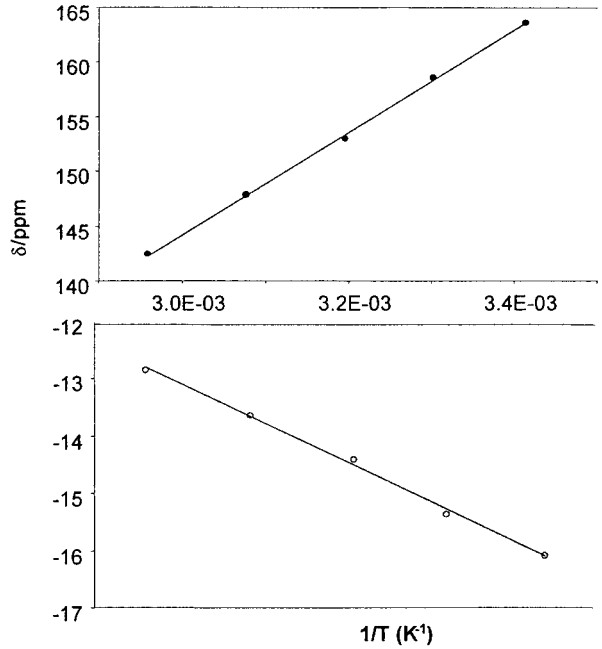

Figure 1. ^{1}H NMR chemical shifts of **6** at different temperatures. Solvent = CD_3CN. Open circles, PMe_3 resonances; solid circles, Cp resonances.

infra). Complex **3** reacts with 0.5 equiv of bromine in toluene at room temperature to afford the expected product, which has been isolated as an analytically pure solid in 70% yield, see eq 5.

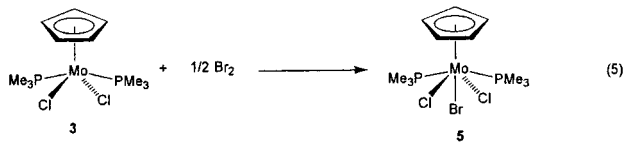

The NMR properties of CD_3CN solutions of **5** show that this compound establishes an equilibrium with the 16-electron complex $CpMo(PMe_3)Cl_2Br$, **6**, and free PMe_3. Diamagnetic compound **5** is characterized by ^{1}H and ^{31}P NMR resonances in the expected ranges (see Experimental Section), analogous to those observed for the trichloride analogue.[63,74] The NMR signals of **6** are paramagnetically shifted, indicating the triplet ground state of this molecule. While the signals of **5** are temperature independent, the resonances of **6** shift with temperature, as expected for a Curie paramagnet (see Figure 1). These properties correspond to those of the trichloride analogues[74,77] and are in full agreement with the results of the theoretical investigation (Scheme 5).

By analogy with the bromination reaction described above for compound **3**, we also attempted to synthesize an analogous derivative from butadiene complex **1**. To our knowledge, no example of a diene complex has been reported so far for Mo(IV). Following a similar procedure to that shown in eq 5 for the phosphine system, a solid was obtained whose NMR spectrum indicates the presence of two products of which one is diamagnetic and the other is paramagnetic. The diamagnetic compound positively contains a diene ligand (three resonances in a 1:1:1 ratio in the expected region) and the Cp ring, while the paramagnetic product shows a broad Cp resonance centered at 183.2 ppm (cf., 179.5 ppm for $[CpMoCl_2(PMe_3)_2]^+$ and 145.4 ppm for $CpMoCl_3(PMe_3)$[74]), and an even larger resonance

Scheme 6

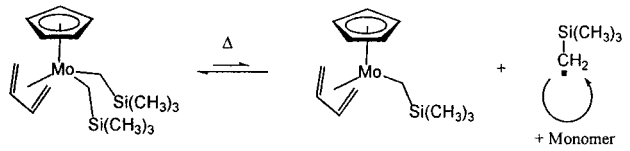

centered at ~14 ppm, presumably resulting from the overlap of all types of butadiene protons. Unfortunately, this compound could not be obtained in an analytically pure form because of its instability. A recrystallization attempt led to crystals of a reduction product, $CpMo(\eta^4\text{-}C_4H_6)Cl_{(2-x)}Br_x$ ($x = 0.28$).[78] This result may be understood on the basis of the reported high oxidation potential of complex **1** (1.25 V higher than that of **3**). Thus, a diene-containing Mo(IV) complex is expected to be a strong oxidant, releasing readily one of its halogen atoms.

C. Controlled Radical Polymerizations. 1. Attempted SFRP with Compound 2. Our first move has been to assess the possibility of controlling the polymerization by using the Mo(II)/Mo(III) redox couple by homolytic cleavage of a Mo(III)−alkyl bond (Scheme 6). For this purpose, compound **2** was heated to 80 °C in the presence of styrene. Under these conditions, no polymerization occurs. This agrees with the high calculated BDE for the Mo−C bond in the model system $CpMo(\eta^4\text{-}C_4H_6)Me_2$ (38.2 kcal/mol, Table 1). At higher temperatures (110 °C), a polymerization process does take place. However, the analysis of the resulting polystyrene reveals that the polymerization is uncontrolled (high molecular weights and broad polydispersities: PDI = 2.6 at 55% conversion). Moreover, this reaction shows similar kinetics to a thermally initiated polymerization at the same temperature (55% vs 52% after 1500 min, respectively).[79,80] If there were control, the free radicals would be primarily trapped under the form of the dormant Mo(III)−alkyl species, and a significant decrease of the polymerization rate would be observed.[81,82] Therefore, as predicted on the basis of the theoretical studies, Mo(III)−alkyl complexes cannot control a radical polymerization by the SFRP protocol, that is, based on the Mo(II)/Mo(III) couple.

2. ATRP with Compounds 3 and 4. The rest of this paper will focus on the redox couple Mo(III)/Mo(IV). We shall first embark on a discussion of the ATRP behavior of Mo(III) complexes. By using **3** or **4** in the presence of (1-bromoethyl)-benzene (BEB) at 80 °C, we observed a controlled radical polymerization (Figure 2, Table S1 in the Supporting Information), as shown by the linear evolution of the M_n with conversion and by the moderate PDIs. Controlled characteristics are also observed with ethyl-2-bromoisobutyrate, BIB, as initiator (Table S1). Faster kinetics are observed with **3** as compared to **4**. The apparent first-order rate constants, as deduced from the slope of $\ln([M]_0/[M])$ versus time plots (Figure 3; [M] signifies the monomer concentration),[83] are equal to the propagation rate constant, k_p, times the free radical concentration. Thus, the free radical concentration is calculated as 1.5 times greater for the polymerization conducted with **3** relative to **4**.

In ATRP, free radicals are produced by the Kharash addition (rate = k'_{-}[Mo(III)][R−Br]) and they disappear by bimolecular

(77) Abugideiri, F.; Gordon, J. C.; Poli, R.; Owens-Waltermire, B. E.; Rheingold, A. L. *Organometallics* **1993**, *12*, 1575−1582.

(78) Le Grognec, E.; Poli, R.; Richard, P. To be published.

(79) Buzanowski, W. C.; Graham, J. D.; Priddy, D. B.; Shero, E. *Polymer* **1992**, *33*, 3055−3059.

(80) Chong, Y. K.; Rizzardo, E.; Solomon, D. H. *J. Am. Chem. Soc.* **1983**, *105*, 7761−7762.

(81) Greszta, D.; Matyjaszewski, K. *Macromolecules* **1996**, *29*, 5239−5240.

(82) Catala, J. M.; Bubel, F.; Hammouch, S. O. *Macromolecules* **1995**, *28*, 8441−8443.

(83) Matyjaszewski, K.; Patten, T. E.; Xia, J. *J. Am. Chem. Soc.* **1997**, *119*, 674−680.

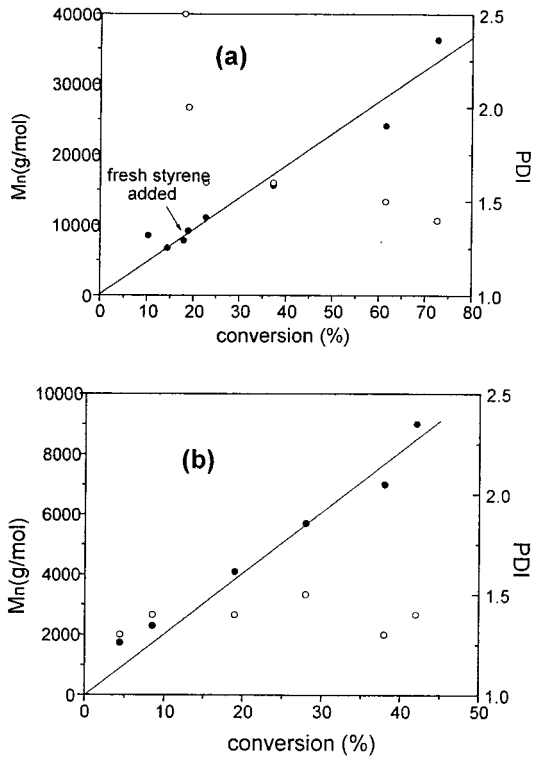

Figure 2. M_n (left axis, solid circles) and PDI (right axis, open symbols) as a function of conversion for the bulk styrene ATRP at 80 °C. (a) With compound **3**, [styrene]/[BEB]/[Mo] = 220(twice)/1/1. (b) With **4**, [styrene]/[BEB]/[Mo] = 270/1/1.

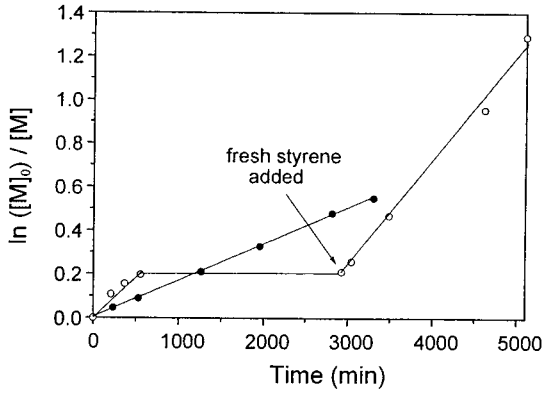

Figure 3. Plots of ln([M_0]/[M]) versus time for the styrene ATRP with **3** (triangles) and **4** (circles). The experiments are the same ones shown in Figure 2.

termination (k_t[R•]^2) and spin trapping reaction (k'_+[Mo(IV)-Br][R•]), see Scheme 2. Therefore, factors favoring an increase in free radical concentration are a low value for k'_+ and/or a high value for k'_-. Equilibrium constants, k'_-/k'_+, may be theoretically calculated for the PH_3 complex and the PH_2CH_2-CH_2PH_2 complexes on the basis of the BDE studies (eqs 3 and 4) and the approximation $\Delta E \approx \Delta H \approx \Delta G$. The values are quite similar for the two systems (8.2×10^{-11} and 5.2×10^{-10}). Yet, the precision of the theoretical calculations prevents us from speculating any further, as a 1.3 kcal/mol difference is smaller than the reliability of this method, especially considering the use of model ligands. Furthermore, the calculations predict a higher radical concentration for the system containing the bidentate ligand, while experimentally the dppe complex **4** gives the slower kinetics.

The equilibrium constants can also be assessed through the use of the redox potentials of **3** (−0.52 V relative to the ferrocene/ferrocenium standard) and **4** (−0.33 V).[84] The reaction of **3** (or **4**) with BEB can be decomposed (see Scheme 7) into the electrochemical oxidation, the bromide coordination to the 16-electron Mo(IV) species, and two additional steps (homolytic rupture of the R−Br initiator and electron affinity of the bromine atom) that are independent of the nature of the organometallic compound. If one assumes that the thermodynamics of the bromide coordination step are not drastically influenced by the nature of the other ligands, then the redox potential is an indication of the position of the redox equilibrium in ATRP.[85] Because **3** is easier to oxidize than **4** by 0.19 V, the radical flux is expected to be more important with **3**, and the polymerization more rapid, as experimentally verified.

Scheme 7

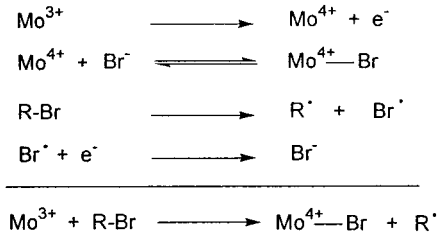

In agreement with a greater radical concentration for the polymerization with **3**, the PRE sets in after ∼15% conversion, as can be observed from Figure 2a and from Figure 3. This is proven by the high molecular weight polymer generated at low conversion, Figure 2a, and by the departure from linearity in the plot of ln([M]$_0$/[M]) versus time at very low conversion, Figure 3. Note that for a radical polymerization controlled by a PRE (in the absence of thermal radical generation), ln([M]$_0$/[M]) is scaling as $t^{2/3}$, but this time dependence is hard to distinguish from a linear time increase.[6,86] At the early stages of the polymerization process, the radical flux is important and is moderated through radical−radical terminations, until the excess of the Mo(IV) spin trap becomes sufficiently important to shift the equilibrium toward the Mo(III) species. Thus, the radicals created at the beginning of the reaction produce dead chains that have the characteristics of an uncontrolled polymerization (for example, during the experiment depicted in Figure 2a, M_n = 78 000 g/mol and PDI = 3 at 2.5% conversion). Note that, at this time, we cannot infer whether k'_+, k'_-, or both values are different for complexes **3** and **4**, because both the k'_-(**3**) > k'_-(**4**) or the k'_+(**3**) < k'_+(**4**) conditions translate into a polymerization rate increase and a departure from the PRE at low conversions.[87]

A controlled character was further assessed by a stop-and-go experiment with **3**, where the polymerization was stopped by cooling at − 20 °C for a day and then restarted after adding a fresh aliquot of styrene (Figure 3). The slope of the ln([M]$_0$/[M]) versus time plot is identical before and after the interruption within experimental error, indicating that the total number of chains is conserved.

Besides gel permeation chromatography (GPC), an analysis of the ATRP polymer has also been carried out using ^{1}H NMR and MALDI-TOF mass spectrometry. The ^{1}H NMR spectrum indicates the presence of bromo terminated chains (δ = 4.35−4.55 ppm for C*H*(Ph)Br in $CDCl_3$),[88] characteristic of chains

(84) Poli, R.; Owens, B. E.; Krueger, S. T.; Rheingold, A. L. *Polyhedron* **1992**, *11*, 2301−2312.

(85) Qiu, J.; Matyjaszewski, K.; Thouin, L.; Amatore, C. *Macromol. Chem. Phys.* **2000**, *201*, 1625−1631.

(86) Souaille, M.; Fischer, H. *Macromolecules* **2000**, *33*, 7378−7394.

(87) Further work concerning the determination of k'_- and k'_+ is in progress.

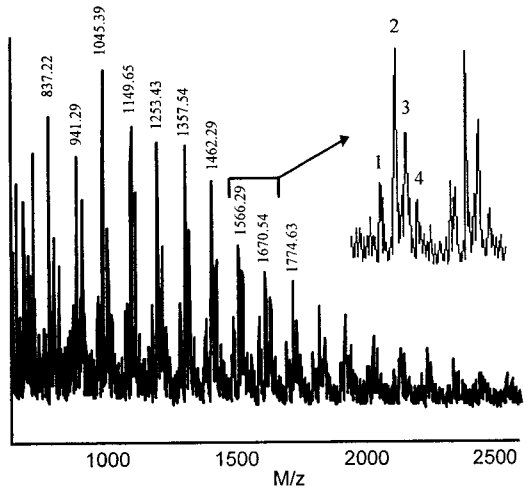

Figure 4. MALDI-TOF mass spectrum of the ATRP polymer. Reaction conditions [Styrene]/[AIBN]/[3] = 200/10/1. Peak 1: $m/z = 1542.77$, $H(Sty)_{12}H_2CH(Ph)BrAg^+$. Peak 2: $m/z = 1566.29$, $H(Sty)_{13}CH{=}CH(Ph)Ag^+$. Peak 3: $m/z = 1585.28$, $H(Sty)_{14}CH{=}CH(Ph)Na^+$. Peak 4: $m/z = 1602.47$, $H(Sty)_{13}CH_2CH(Ph)ClAg^+$.

obtained through an ATRP mechanism. The MALDI-TOF spectrum (Figure 4) shows four families of peaks. The main peaks correspond to analyte having the formula $(C_6H_5)CH(CH_3)(C_8H_8)_nC(C_6H_5){=}CH_2Ag^+$. As vinyl-terminated end-group resonances are not observed in the NMR, we believe that these species correspond to bromo terminated chains that have undergone a dehydrobromination process upon contact with the silver salt. The second set of peaks matches the molecular formula $(C_6H_5)CH(CH_3)(C_8H_8)_nCH(C_6H_5)CH_2BrAg^+$, namely the dormant chains. The third set of peaks are due to $(C_6H_5)CH(CH_3)(C_8H_8)_nC(C_6H_5){=}CH_2Na^+$, with the sodium ions originating from the usual impurities contaminating the sample.[89,90] Finally, the last set of peaks corresponds to the formula $(C_6H_5)CH(CH_3)(C_8H_8)_nCH(C_6H_5)CH_2ClAg^+$. Although the Mo−Br bond is weaker than the Mo−Cl bond (see eq 2 for BDEs), the radical selectivity is evidently not 100% in favor of the abstraction of Br. Thus, a very small proportion (not quantified by MALDI-TOF mass spectrometry) of dormant chains are Cl terminated. Because of their low abundance, the chloro terminated chains are not observed by NMR.[91,92]

A supplementary element to confirm the ATRP mechanism lies in the possibility to effect so-called reverse ATRP. Starting from the aforementioned $CpMoCl_2Br(PMe_3)_2$, **5**, and a suitable radical source (2,2′-azobisisobutyronitrile, AIBN) at 90 °C, the polymerization of styrene is found to be controlled, as shown by the linear evolution of M_n versus conversion (Figure 5 and Table S2) and moderate PDI. Contrary to direct ATRP, there is no delay to reach PRE equilibrium: molecular weights correspond to the theoretical values even at low conversions. Note that the reaction was conducted at 90 °C in order to have a rapid initiation (AIBN decomposition) relative to the propagation ($t_{1/2}$ for AIBN is 17 min at this temperature).[93] Because of this high temperature (direct ATRP was carried out at 80°C), the level of control is lower than that for the direct experiments. As a result, PDIs are consistently above 1.5.

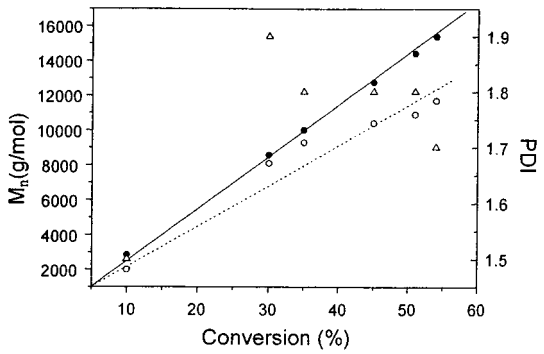

Figure 5. M_n (circles, solid for theoretical values and open for experimental) and PDI (triangles) in reverse ATRP with **5**. Reaction conditions [Styrene]/[AIBN]/[**5**] = 270/1.5/1.

Attempts to polymerize methyl methacrylate (MMA) in bulk or in solution (10% in chlorobenzene) with compound **3** initiated with BIB at temperatures ranging from 40 to 100 °C do not result in controlled polymerization. Kinetics are found to be very rapid and related to uncontrolled polymerization kinetics. For example, in the bulk at 65 °C, 50% conversion is reached after 200 min, with a very pronounced Trommsdorff effect, followed by a complete vitrification around 90% conversion. Molecular weights are elevated throughout polymerization and are decreasing with conversion because of the Trommsdorff effect. We believe that the halogenated compound reacts with the Mo(III) complex to generate radicals, thus triggering the polymerization, but the tertiary propagating radicals are too bulky to interact with the spin trap. The MALDI-TOF mass spectrum of the PMMA sample exhibits two families of peaks corresponding to $(CH_3)_2C(COOEt)(CH_2C(COOMe)(Me))_n(CH_2C(COOMe)({=}CH_2))$ and $(CH_3)_2C(COOEt)(CH_2C(COOMe)(Me))_n(CH_2C(COOMe)(CH_3))$, that is to say, chains that are initiated by BIB and terminated through disproportionation as usually observed for MMA.[94]

3. SFRP with Compounds 1, 3, and 4. It is usually accepted that, in ATRP, there is no direct metal−carbon bond formation between the radical and the metal complex.[95] However, with complexes **1**−**4**, theoretical calculations indicate that the oxidative pathway through halogen transfer is energetically competitive with the organometallic bond formation with a propagating free radical [cf. eqs 2 (X = CH_3) and 3−4]. Thus, when both Mo(III) and Mo(IV)−Br complexes are present, a choice is offered to the radical. Before embarking on a discussion of the reaction scheme when both routes are simultaneously present, the behavior of Mo(III) complexes with free radicals has been assessed in an SFRP process whereby the radical is initially produced from AIBN. To our surprise, we found that systems **1**−**4**/AIBN are efficient in the SFRP polymerization of styrene at temperatures as low as 80 °C. At 100 °C, the half-life of AIBN is less than 15 min (vide supra), whereas the polymerization lasts several hours, thus ensuring that the radical generation step is ended at the early instants of the polymerization (initiation is fast relative to propagation). A linear increase of M_n versus conversion (Figure 6 and Table S3) and moderate PDIs (1.3−1.7 for the polymerization with compounds **1** and **4**) are pointing toward controlled behavior. M_n is consistently

(88) Matyjaszewski, K.; Coca, S.; Nakagawa, Y.; Xia, J. *Polym. Mater. Sci. Eng.* **1997**, *76*, 147−162.
(89) Dourges, M. A.; Charleux, B.; Vairon, J.-P.; Blais, J.-C.; Bolbach, G.; Tabet, J.-C. *Macromolecules* **1999**, *32*, 2495−2502.
(90) Bednarek, M.; Biedroni, T.; Kubisa, P. *Macromol. Chem. Phys.* **2000**, *201*, 58−66.
(91) Beers, K. L.; Kern, A.; Matyjaszewski, K. *Polym. Prepr. (Am. Chem. Soc., Div. Polym. Chem.)* **1997**, *38*, 693.
(92) Nakagawa, Y.; Gaynor, S.; Matyjaszewski, K. *Polym. Prepr. (Am. Chem. Soc., Div. Polym. Chem.)* **1996**, *37*, 577−578.
(93) Bandrup, J.; Immergut, E. H. *Polymer Handbook*; Wiley: New York, 1992.
(94) Moad, G.; Solomon, D. H. *The Chemistry of Free Radical Polymerization*; Pergamon: Oxford, 1995.
(95) Matyjaszewski, K.; Woodworth, B. E. *Macromolecules* **1998**, *31*, 4718−4723.

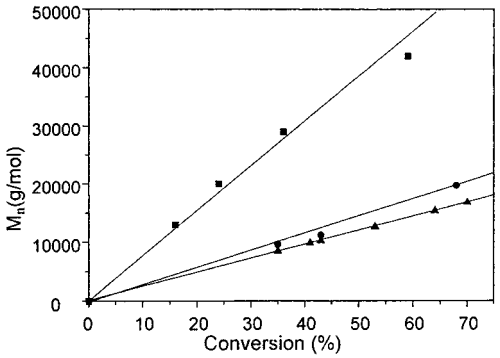

Figure 6. M_n versus conversion for the bulk styrene SFRP at 100 °C. Squares [styrene]/[AIBN]/[**1**] = 188/0.33/1. Circles [styrene]/[AIBN]/[**3**] = 223/0.78/1. Triangles [styrene]/[AIBN]/[**4**] = 230/0.80/1.

higher than the theoretical molecular weight, indicating that the initiation efficiency is lower than 1 (0.25 for **1**, 0.70 for **3**, and 0.75 for **4**). The low efficiency is due to the unproductive AIBN decomposition (initial radical loss through recombination by cage effect), as the efficiencies (0.25, 0.70, 0.75) are proportional to the amount of AIBN relative to the Mo complex (0.33, 0.78, 0.80). It should also be pointed out that molecular weight analyses (by GPC) are carried out in air; clearly, the metallorganic end groups would not remain intact under such conditions, and dead polymer could possibly be formed through radical−radical coupling or oxygen-mediated radical oxidation as soon as the reaction mixture is exposed to air,[89] thus explaining the discrepancy between theoretical and experimental molecular weights.

In the SFRP mechanism, the interaction between Mo(III) and the free radical generates a Mo(IV) alkyl chloride complex that putatively reversibly dissociates. However, as it has been shown here that free radicals react through an atom transfer pathway with Mo(IV) halides, it is also conceivable that the free radicals react with the initially generated Mo(IV) alkyl chloride in our systems: the observed control would then arise from an ATRP scheme. Our experimental evidence allows us to rule out such a mechanism. The ^{1}H NMR of the isolated polymer obtained from an SFRP experiment (159 mg of **1**, 12 mL of styrene, and 30 mg of AIBN; T = 100 °C; time = 353 min; M_n = 42 000 g/mol; PDI = 1.6) does not indicate the presence of chlorinated end groups. Possibly, the putative spin trap (Mo(IV)X_2R, R = polymer chain) is extremely bulky and unlikely to react rapidly with another bulky macroradical. Another possible event to be considered is halogen atom abstraction by the free radical from Mo(III), to generate a dormant halide and a Mo(II) complex. This possibility, however, can be discarded outright, not only because we do not observe chlorinated end groups, as stated, but also because the Mo(III)−Cl bond is too strong, according to the calculations (Table 1), for this process to be thermodynamically viable.

As shown by the average PDIs and limited conversions, the polymerization is not exempt from termination/transfer reactions. After a few hours, the rate of radical termination is exactly balanced by the rate of generation of thermal radicals, as observed in numerous other cases.[66,67,81,82,96,97] Possible chain ending reactions include free radical coupling or disproportionation and β-hydride abstraction at the Mo(III) active center through bimolecular transfer reaction between a free radical and an SFR (vide supra), as in cobalt systems.[14,42] The presence and the role of the Mo(IV) hydride will be discussed below.

Table 4. Attempted ATRP Polymerization of Styrene with Complexes **1** and **2** in Bulk

complex	[MON]/[BEB]	[BEB]/[Mo]	time (min)	conversion (%)	M_n (g/mol)	PDI
1[b]	196	1	77	9	1200	1.4
1[b]	196	1	135	16	1200	1.4
1[b]	196	1	195	21	1200	1.4
1[b]	196	1	320	29	1200	1.4
1[b]	196	1	2680	63	1400	1.5
1[b]	200	10	60	8	1500	2.5
1[b]	200	10	120	15	1400	1.4
1[b]	200	10	190	26	1300	1.4
1[b]	200	10	550	46	1400	1.5
1[b]	200	10	1140	67	1600	1.6
1[b]	200	10	1775	72	1600	1.7
2[a]	250	10	55	25	1800	1.7
2[a]	250	10	150	30	1300	1.6
2[a]	250	10	275	35	1500	1.7
2[a]	250	10	1275	48	1400	1.6

[a] At 80 °C. [b] At 100 °C.

4. Aborted ATRP with Compounds 1 and 2. To our surprise, ATRP experiments conducted with **1** or **2** only resulted in the generation of small oligomers, with molecular weights independent of conversion (Table 4). The number of polymer chains generated in this system is far greater than the amount of initiator, thus indicating that transfer occurs. Transfer to solvent or to monomer and styrene self-initiation cannot be responsible for such behavior because, if that were the case, low molecular weights would also be constantly observed for polymerizations performed in the presence of **3** and **4**. A catalytic chain transfer (CCT) mechanism must be invoked to accommodate these data.[40,98−101] The presence of CCT is also confirmed by NMR and MALDI-TOF analyses of the oligomers. The ^{1}H NMR analysis of the polymers indicates end-group resonances located between 6.05 and 6.35 ppm (in $CDCl_3$), resonances that are typical of vinylidene protons created through β-elimination in CCT. In the MALDI-TOF mass spectrum of PS (Figure 7), separate oligomers are clearly resolved and separated by 104 m/z corresponding to the mass of styrene. This family of peaks corresponds to the expected product, where one extremity is the H group and the other is PhCH═CH. No other products can be observed in the spectrum.

How are we to explain that, in SFRP with **1**, polymerization occurs with little or no transfer, whereas, under ATRP conditions, CCT is observed? First, the fact that radical polymerization occurs at a significant rate in the ATRP experiment is in agreement with the presence of an initial radical generating reaction (reaction a in Scheme 8). The free radical propagates (reaction b), until it reacts with a spin trap. The spin trap can be the Mo(III) complex (reaction c), as seen previously in the SFRP section, or a Mo(IV) halide complex, if an ATRP scheme is also prevailing (reaction a). However, an intermolecular transfer between the propagating radical and the Mo(III) complex can also occur as in CCT (reaction d).[42,102] The difference between the SFRP experiment and the "aborted"

(96) Ohno, K.; Tsujii, Y.; Fukuda, T. *Macromolecules* **1997**, *30*, 2503−2506.
(97) Hammouch, S. O.; Catala, J.-M. *Polym. Prepr. (Am. Chem. Soc., Div. Polym. Chem.)* **1997**, *38*, 655−656.
(98) Haddleton, D. H.; Maloney, D. R.; Suddaby, R. K. *Macromolecules* **1996**, *29*, 2229−2232.
(99) Haddleton, D. M.; Maloney, D. R.; Suddaby, K. G.; Muir, A.; Richards, S. N. *Macromol. Symp.* **1996**, *111*, 37.
(100) Heuts, J. P. A.; Kukulj, D.; Forster, D. J.; Davis, T. P. *Macromolecules* **1998**, *31*, 2894−2905.
(101) Sanayei, R. A.; O'Driscoll, K. F. *J. Macromol. Sci., Chem.* **1989**, *A26*, 1137−1149.
(102) Gridnev, A. A.; Ittel, S. D.; Fryd, M.; Wayland, B. B. *Organometallics* **1996**, *15*, 222−235.

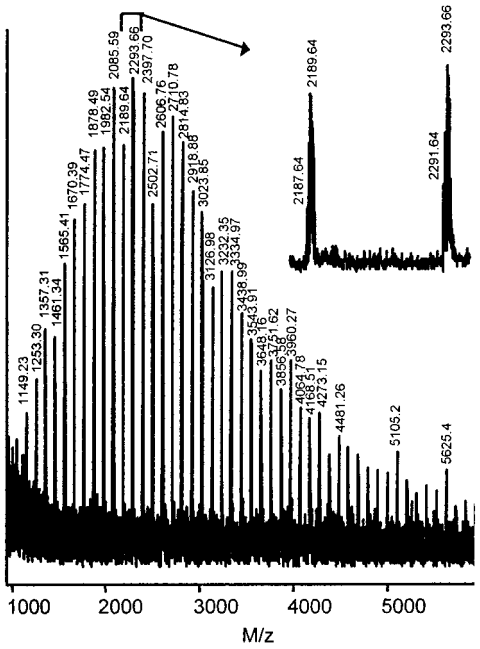

Figure 7. MALDI-TOF mass spectrum of the CCT polymer. Reaction conditions [Styrene]/[BEB]/[1] = 200/1/1 at 80 °C.

Scheme 8

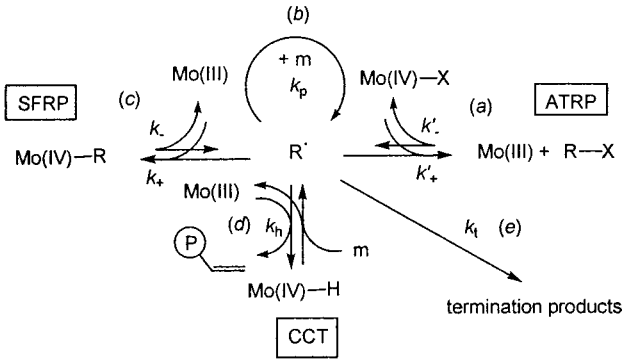

ATRP experiment lies in the molecular weight distribution. The instantaneous number average molecular weight is the ratio of the propagation rate to the chain stopping events and can be expressed in eq 6,[103] where M_0 is the monomer molecular weight, [m] is the monomer concentration, and [R•] is the total free radical concentration.

$$M_n = M_0 \frac{k_p[m]}{k_t[R^\bullet] + k_h[Mo(III)]} \qquad (6)$$

Obviously, the molecular weight decreases as the concentration of spin trap Mo(III) increases. In the SFRP experiment, the Mo(III)/Mo(IV) ratio is mostly regulated by equilibrium c, which is exothermic in the direction of Mo(III) *consumption* (cf., eq 2), while in the ATRP experiment it is regulated by equilibrium a, which is exothermic in the direction of Mo(III) *production* (cf., eqs 3−4).[104] Thus, [Mo(III)] will be much higher in the ATRP experiment, resulting in a much more favorable chain transfer. To further clarify this point, we have simulated the polymerization kinetics for an SFRP experiment with **1** and for an ATRP experiment with **1**, where chain transfer (process d of Scheme 8) was deliberately allowed. The simulations were run for different chain transfer constants ($C_{tr} = k_h/k_p$), see the Supporting Information for details. The numerical values of all other necessary rate constants (AIBN decomposition, k_i; propagation, k_p; termination by coupling, k_t; radical formation by thermal initiation, k_{is}) were obtained from literature sources.[105] At 100 °C, these are the following: $k_i = 1.864 \times 10^{-3}$ s^{-1}, $k_p = 1245$ s^{-1} mol^{-1} L, $k_t = 1.33 \times 10^8$ s^{-1} mol^{-1} L, $k_{is} = 2 \times 10^{-10}$ s^{-1} mol^{-2} L^2, and $f = 0.8$. The values for k_+, k_-, k'_+, and k'_- ($k_+ = 3 \times 10^7$ L mol^{-1} s^{-1}, $k_- = 1$ s^{-1}, $k'_+ = 3 \times 10^7$ L mol^{-1} s^{-1}, and $k'_- = 1$ L mol^{-1} s^{-1}) have been chosen according to Table 5. For a wide range of C_{tr} values, the molecular weight versus conversion plot in SFRP (up to 50% conversion) is close to linear, see Figure 8. Under ATRP conditions, on the other hand, and for the same range of C_{tr} values, the molecular weight becomes essentially conversion-independent and remains small, as typically observed in CCT, for the higher transfer constants (Figure 9).

Table 5. Relevant Energetic Parameters for Complexes **1**, **3**, and **4**

complex	ΔG(SFRP) (kcal/mol)	ΔG(ATRP) (kcal/mol)	C_{tr}
1	−12.8	12.8	5.0
3	−11.8	12.2	0.3
4	−12.1	12.6	0.8

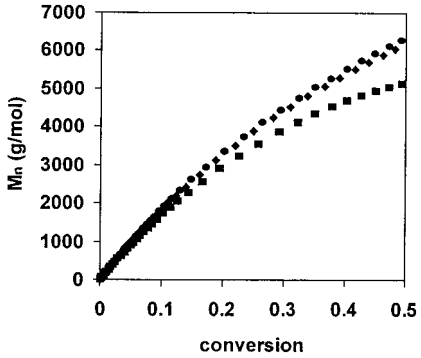

Figure 8. Plot of M_n versus conversion for a simulated SFRP polymerization with β-hydride transfer at 100 °C. Circles, $C_{tr} = 0.1$; diamonds, $C_{tr} = 1$; squares, $C_{tr} = 8$. Simulation conditions: [**1**] = [AIBN] = 0.0409 mol L^{-1}; [styrene] = 7.69 mol L^{-1}, $k_+ = 3 \times 10^7$ s^{-1} mol^{-1} L; $k_- = 1$ s^{-1}. For other conditions, see text.

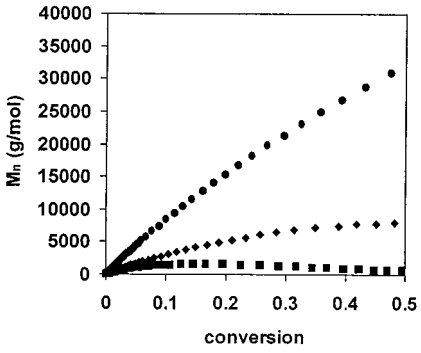

Figure 9. Plot of M_n versus conversion for a simulated ATRP polymerization with β-hydride transfer. Circles, $C_{tr} = 0.1$; diamonds, $C_{tr} = 1$; squares, $C_{tr} = 8$. Simulation conditions: [RBr] = 0.05 mol L^{-1}, $k'_+ = 3 \times 10^7$ s^{-1} mol^{-1} L; $k'_- = 1$ s^{-1} mol^{-1} L. Other conditions are as for Figure 8.

D. Differences/Similarities between 1, 2, 3, and 4. The last question that remains to be addressed is why, although compounds **1** and **2** yield CCT polymerization under ATRP conditions, compounds **3** and **4** do not. Indeed, the same

(103) Dotson, N. A.; Galvan, R.; Laurence, R. L.; Tirrell, M. *Polymerization Process Modeling*; VCH: New York, 1995.

(104) The calculations on the related Mo(III)−CH_3 BDE show that the energetics are little affected by the nature of the other coligands.

(105) Herk, A. M. V. *J. Macromol. Sci., Rev. Macromol. Chem. Phys.* **1997**, *C37*, 633−648.

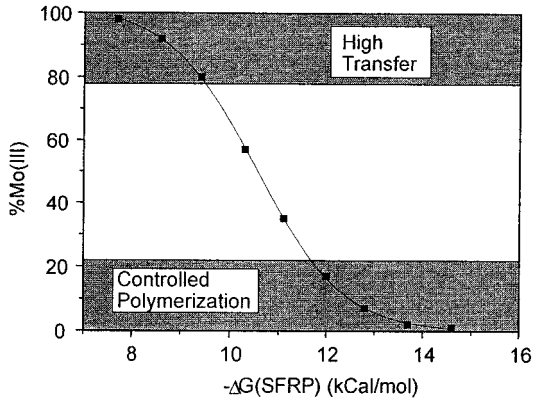

Figure 10. Relative amount of Mo(III) at 50% conversion in an SFRP experiment ($T = 100$ °C) versus the position of the SFRP equilibrium, i.e., $-RT \ln(k_+/k_-)$ in Scheme 8c. Simulation conditions are as in Figure 8.

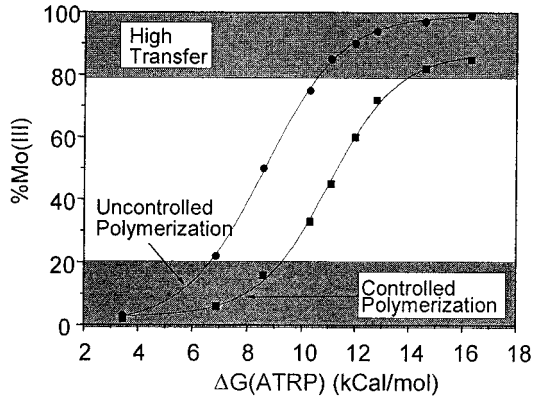

Figure 11. Relative amount of Mo(III) at 50% conversion in an ATRP experiment ($T = 100$ °C) versus the position of the ATRP equilibrium, i.e., $-RT \ln(k'_-/k'_+)$ in Scheme 8d). Squares, ΔG(SFRP) −12.8 kcal/mol; circles, ΔG(SFRP) = −9.4 kcal/mol. Simulation conditions are as in Figure 9.

considerations made above concerning the [Mo(III)]/[Mo(IV)] dependence on polymerization conditions should be applicable to compounds **3** and **4**. The detailed examination of the polymerization scheme indicates that a minute change in the nature of the complex can direct the reaction toward all possible mechanisms. As such, the efficiency of a particular complex in SFRP, ATRP, or CCT does not seem to be the consequence of a single factor (redox potential, magnetic moment, complex bulkiness, nature of the metallic SOMO, etc.), but rather the result of steep kinetic equations that prevail in radical chemistry. Thus, the intimate nature of the coordination sphere may influence the living/transfer outcome of styrene polymerization under ATRP conditions. It is convenient to first briefly reexamine the polymerization under SFRP conditions with the aid of further simulations.

For complexes **1**, **3**, and **4**, it is possible to observe an SFRP controlled behavior, even in the presence of β-hydride transfer. In Figure 10, the amount of Mo(III) (at 50% monomer conversion) has been plotted for different values of the Mo(IV)−alkyl bond strength in the presence of chain transfer ($C_{tr} = 8$). As chain transfer does not affect the overall radical concentration, this plot is independent of C_{tr}. Indeed, in Scheme 8 (process d), the reaction of the hydride complex with an olefin is known to be faster than the reverse olefin elimination (k_h), as the metallic hydride has never been observed or isolated;[39,42] thus, the catalytic transfer reaction is not influencing the Mo(III) and radical concentrations. Controlled polymerization[106] is observed for $-\Delta G \geq 12$ kcal/mol (low transfer, slow kinetics, PDI ≤ 1.5), whereas CCT is observed for $-\Delta G \leq 10$ kcal/mol (high transfer, little retardation, PDI ~ 2). It is noteworthy that only a 2 kcal/mol difference is sufficient to switch the system from "living" SFRP to CCT. In our case, the BDE for $CpMoCl_2(PH_3)_2-CH_3$ was calculated as 24.3 kcal/mol (see section A), far above 12 kcal/mol. Note, however, that a lower BDE is to be expected for the actual experimental systems (e.g., $CpMoCl_2(PMe_3)_2-CHEtPh$), because of the steric compression and the stabilization of the resulting radical. An additional argument hints toward a lower BDE: for a value as high as 24.3 kcal/mol, the simulation results suggest that that polymerization should stop at around 50% conversion, because of the accumulation of the spin trap (PRE effect). The kinetics that we show in Figure 6 for **1** seem consistent with a BDE of 12.8 kcal/mol (see Table 5).

We now move on to the analysis of the polymerization run under ATRP conditions. With the proviso that the SFRP mechanism can occur simultaneously, the situation is further complicated by the additional process a in Scheme 8, relative to the pure SFRP situation examined above. In the absence of β-H transfer, it is clear that the polymerization will always be controlled, provided the ΔG(SFRP) is sufficiently high, notwithstanding the position of the ATRP equilibrium. For example, for the very weak redox equilibrium ΔG(ATRP) $= -RT \ln(k'_-/k'_+) = 9.2$ kcal/mol (ΔG(SFRP) $= -12.8$ kcal/mol), the simulation of the styrene polymerization kinetics at 110 °C indicates a linear growth of the molecular weight with conversion (80% in 12 h) and a final PDI of 1.4. Higher values for ΔG(ATRP) result in more controlled behavior and slower kinetics. In the presence of β-H transfer ($C_{tr} = 8$), the outcome of the polymerization has been graphically depicted in Figure 11 for two different positions of the SFRP equilibrium. High values for ΔG(ATRP) result in slow kinetics and a massive generation of oligomers through CCT. For ΔG(SFRP) $= -12.8$ kcal/mol (complex **1**), transfer predominates when ΔG(ATRP) ≥ 12 kcal/mol, whereas the same situation is verified at a lower ΔG(ATRP) (≥ 10 kcal/mol) when ΔG(SFRP) is less negative (−9.4 kcal/mol). For low values of ΔG(ATRP), the redox ATRP equilibrium is strongly shifted toward the radical generation side. In this case, the outcome of the polymerization depends on the SFRP equilibrium. If $-\Delta G$(SFRP) is low, neither the SFRP nor the ATRP equilibria are able to control the radical flux: an uncontrolled polymerization is observed. For high $-\Delta G$(SFRP), a controlled SFRP-type polymerization is observed, albeit radicals are generated through an atom transfer reaction. Once again, it is noteworthy that just a slight decrease in ΔG(ATRP) (2 kcal/mol) translates into a bifurcation from CCT to controlled polymerization (high ΔG(SFRP)) or to uncontrolled polymerization (low ΔG(SFRP)).

The values of ΔG(ATRP), ΔG(SFRP), and C_{tr} have been obtained by trial and error curve fitting of the experimental kinetics (Figure 12 and Table 5). With the set of values we have chosen, the fit is excellent for conversion curves (ATRP and SFRP experiments) and molecular weight curves (ATRP experiments only; for SFRP, see above). The main problem with this approach is that more than one set of values could

(106) The limit between controlled and uncontrolled polymerization has been arbitrarily set at 20% Mo(III) at 50% conversion. For example, for the polymerization depicted in Figure 8 (circles), there is 17% Mo(III) at 50% conversion. Molecular weight grows linearly with conversion and differs by 5% from the "theoretical" value: $MW_0 \cdot \text{conversion} \cdot [\text{Monomer}]_0/[\text{Mo}]_0$. PDI at 50% conversion is found to be 1.16. The experimentalist would consider this a controlled polymerization. The lower the amount of Mo(III), the more controlled the polymerization and the slower the polymerization.

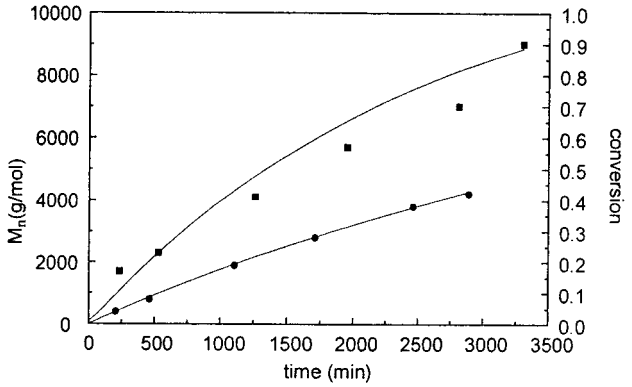

Figure 12. Experimental molecular weights (square) and conversions (circles) versus time for the ATRP of styrene with **4**. The experimental values correspond to entries 1−6 of the Supporting Information Table S1. The plain lines correspond to the simulated values using ΔG(SFRP) = −12.1 kcal/mol, ΔG(ATRP) = +12.6 kcal/mol, C_{tr} = 0.8.

conceivably fit the experimental data. Keeping in mind this limitation, we have found that the energetic parameters are relatively close to each other. For instance, the chain transfer constants differ only by 1 order of magnitude. The ΔG(ATRP) values for $CpMoCl_2(PH_3)_2$ and $CpMoCl_2(PH_2CH_2CH_2PH_2)$ have been calculated as 16.3 and 15.0 kcal/mol, respectively (see section A). We could therefore expect that **3** and **4** are potential CCT promoters, according to Figure 11. We can rationalize the obvious discrepancy with the experimental results by proposing that the use of model phosphine PH_3 in the computational studies leads to an overestimation of the ΔG(ATRP) values, for steric reasons. The decrease of BDEs following an increase of steric pressure is a well-known and general occurrence. This phenomenon will be more critical for the PMe_3 and dppe ligands of compounds **3** and **4**, while the butadiene ligand in compound **1** is much less sterically encumbering and should therefore negatively affect the ΔG(ATRP) value to a much lesser extent. Furthermore, the steric bulk of the same ligand is also expected to negatively affect the β-hydrogen transfer rate, k_h (i.e., process d of Scheme 8), by preventing the approach of the free radical.[14] The values of k_h for the different compounds **1**−**4** were not experimentally measured, nor were they theoretically calculated in the present investigation. Further work in our laboratory is aimed at clarifying this point.

Summary

Several conclusions can be drawn from these mechanistic studies. The key findings are as follows:

1. The same complex (such as **3** or **4**) can be efficient in SFRP or in ATRP. Under ATRP conditions, the radical concentration is potentially regulated by both the atom transfer reaction and by the reversible termination to Mo(III) (two distinct PRE effects). This should be contrasted with Cu(I) mediated ATRP, where it has been proven that only atom transfer reaction occurs.[95] Future work will concentrate on quantifying the amount of SFRP versus ATRP.

2. Mo(III) complex **1** is a modest CCT catalyst for the polymerization of styrene ($C_{tr} \sim 5$). To our knowledge, this is the first time that a non-cobalt based CCT has been reported.

3. The same complex can activate SFRP and ATRP controlled polymerization processes, provided the chain transfer reaction is not important. For the complexes studied in this work, this is the case when $C_{tr} \leq 1$ (Table 5). When $C_{tr} \geq 1$, a CCT process can be observed, if the polymerization is carried out with high concentrations of Mo(III) (as in the case of the aborted ATRP experiment). However, the CCT mechanism can be occulted if the Mo−alkyl bond is sufficiently strong: kinetics simulations indicate that only 2 kcal/mol separates the BDE of an SFRP promoter to the BDE of a CCT catalyst.

In a more general sense, the present work has provided a basis for the utilization of thermochemical considerations (bond dissociation energies), in conjunction with a global kinetic model, to understand and predict the ability of a particular metal system to control the radical polymerization of a particular monomer in "living" or CCT manners.

Experimental Section

General Procedures. All reactions were carried out in a Jacomex glovebox or by the use of standard Schlenk techniques under an argon atmosphere. Styrene was washed by a NaOH aq solution (10%), neutralized with water, dried with $MgSO_4$, and then distilled at 25 °C under reduced pressure. Toluene, diethyl ether, THF, and pentane were purified by distillation under argon after drying over sodium benzophenone ketyl. ^{1}H NMR measurements were carried out on a Bruker AC200 spectrometer. The peak positions are reported with positive shifts in ppm downfield of TMS, as calculated from the residual solvent peaks. Elemental analyses were performed with a Fisons EA 1108 apparatus. MALDI-TOF mass spectrometric analyses were carried out on a Perkin-Elmer Voyager-DE STR. In a typical run, the polymers were dissolved in THF (10 g/l) and then mixed with the matrix (Dithranol). PS samples were cationized with silver salt, and PMMA with sodium salt. GPC separations were conducted on a Waters apparatus using THF as eluent (1 mL/min) and equipped with a refractometer, a diode array UV−vis spectrophotometer, light-scattering Wyatt MiniDawn detectors, and five separation columns from UltraStyragel Waters. Compounds **1**−**4** were obtained according to previously described synthetic procedures.[49,54,72,107] (1-Bromoethyl)benzene and ethyl-2-bromoisobutyrate were purchased from Aldrich Chemical Co. and degassed before use. Azobisisobutyronitrile (JANSSEN) was recrystallized twice from MeOH before use.

Synthesis of $CpMo(PMe_3)_2Cl_2Br$, 5. A toluene solution (5 mL) of **3** (76 mg; 0.197 mmol) was prepared. Br_2 (5 μL; 15.8 mg; 0.098 mmol) was added by microsyringe under vigorous stirring. The reaction is immediate, yielding the product as a red-brown precipitate. The formed suspension was stirred for an additional 15 min. The supernatant was cannulated off, and the product was washed with 2 × 5 mL of diethyl ether, then washed with 2 × 5 mL of pentane, and finally dried in vacuo. Yield = 64 mg, 70%. Anal. Calcd for $C_{11}H_{23}BrCl_2Mo$: C, 28.47; H, 4.99. Found: C, 28.24; H, 5.12. In solution, compound **5** establishes an equilibrium with **6** and free PMe_3. The NMR spectra of an aliquot after evaporation to dryness and dissolution in CD_3CN show the presence of both complexes. ^{1}H NMR (CD_3CN, 20 °C, δ) complex **5**: 1.8 (s, 18H, $P(CH_3)_3$), 4.1 (s, 5H, C_5H_5). Complex **6**: −16 (s, br, $\omega_{1/2}$ = 340 Hz, 9H, $P(CH_3)_3$), 164 (s, br, $\omega_{1/2}$ = 300 Hz, 5H, C_5H_5). No signals were observed by ^{13}C NMR after 40 000 accumulations.

Reaction of $CpMo(\eta^4\text{-}C_4H_6)Cl_2$, 1, with Br_2. To a suspension of **1** (100 mg; 0,35 mmol) in 7 mL of toluene was added 9 μL of Br_2 (0.17 mmol) by microsyringe under vigorous stirring. An immediate reaction yields a brown precipitate. The mother liquor was eliminated via a cannula, and the product was washed with 3 × 35 mL of ether and dried under vacuum. This material did not analyze correctly for a Mo(IV) product of stoichiometry $CpMo(\eta^4\text{-}C_4H_6)Cl_2Br$. The ^{1}H NMR spectrum ($CDCl_3$, 20 °C, δ) exhibits peaks due to a diamagnetic and a paramagnetic product. Diamagnetic product: 1.1 (m, 2H, C_4H_6), 1.9 (m, 2H, C_4H_6), 3.6 (m, 2H, C_4H_6), 3.95 (s, 5H, C_5H_5). Paramagnetic product: 14 (s, br, $\omega_{1/2}$ = 325 Hz, C_4H_6), 183.2 (s, br, $\omega_{1/2}$ = 290 Hz, C_5H_5). A recrystallization from CH_2Cl_2/pentane afforded crystals of a decomposition product, shown by X-ray diffraction to correspond to $CpMo(\eta^4\text{-}C_4H_6)Cl_{(2-x)}Br_x$ (x = 0.28).[78] Anal. Calcd for $C_9H_{11}Br_{0.28}Cl_{1.72}Mo$: C, 36.21; H, 3.71. Found: C; 35.91; H, 3.56.

ATRP Polymerizations. All ATRP polymerization reactions were conducted following the same experimental procedure. A typical procedure is described as a representative example. Complex **4** (141

(107) Linck, R. G.; Owens, B. E.; Poli, R.; Rheingold, A. L. *Gazz. Chim. Ital.* **1991**, *121*, 163−168.

mg, 0.22 mmol) was added to a 25 mL Schlenk tube equipped with a stirring bar. Styrene (7 mL, 61 mmol) and 1-bromo-1-phenylethane (30 μL, 0.22 mmol) were added to the reaction flask by a syringe after a 20 min Ar purge. The Schlenk tube was then immersed in an oil bath heated at 80 °C. Aliquots were withdrawn periodically for a reaction monitoring by GPC.

SFRP Polymerizations. All SFRP polymerizations were conducted following the same experimental procedure. A typical procedure is described here as a representative example. Complex **1** (159 mg, 0.55 mmol) and AIBN (30 mg, 0.18 mmol) were added to a 25 mL Schlenk tube equipped with a stirring bar. Styrene (12 mL, 104 mmol) was then added by a syringe, and the Schlenk tube was immersed in a oil bath heated at 100 °C. Aliquots were withdrawn periodically for reaction monitoring by GPC.

Computational Investigations. All calculations were performed using Gaussian 94[108] on an SGI Origin200 workstation. The LANL2DZ basis set was employed to perform geometry optimizations with a DFT approach. The three parameter form of the Becke, Lee, Yang, and Parr functional (B3LYP)[109] was used in all cases. The energies reported for the open shell (doublet and triplet) systems correspond to unrestricted B3LYP calculations. The mean value of the first-order wave function, which is not an exact eigenstate of S^2 for unrestricted calculations on the open-shell systems, was considered suitable for the unambiguous identification of the spin state. Spin contamination was carefully monitored, and the values of $\langle S^2 \rangle$ for the unrestricted B3LYP systems at convergence were very close to the ideal value of 0.75 for doublets and 2.0 for triplets.

Kinetics Modeling. The kinetic equations were written for all nonpolymeric species (Mo(III), Mo(IV)-Br, RBr, AIBN) and for the zeroth, first, and second moments of the radical, dead, and dormant chains.[103] These equations are available in the Supporting Information. The set of differential equations was solved with the commercial Matlab Software (version 5.1). Number and weight average polymerization degrees were obtained as the ratios of first to zeroth and second to first moments, respectively.

Acknowledgment. The authors are grateful to the CNRS (Program Catalyze pour l'Industrie et l'Environnement), the Conseil Régional de Bourgogne, and COST D17 (Working group on Transition Metal Mediated Living Radical Polymerization) for supporting this work and CINES for free computational time. E.L.G. thanks the MENRT for the Ph.D. fellowship. In addition, we thank C. Novat for GPC expertise and F. Delolme and G. Dessalces for MALDI-TOF analyses.

Supporting Information Available: Tables S1−S3 of ATRP, reverse ATRP, and SFRP polymerization results; detailed description of the modeling of the SFRP + CCT and the SFRP + ATRP + CCT processes (PDF). This material is available free of charge via the Internet at http://pubs.acs.org.

JA010998D

(108) Frisch, M. J.; Trucks, G. W.; Schlegel, H. B.; Gill, P. M. W.; Johnson, B. G.; Robb, M. A.; Cheeseman, J. R.; Keith, T. A.; Petersson, G. A.; Montgomery, J. A.; Raghavachari, K.; Al-Laham, M. A.; Zakrzewski, V. G.; Ortiz, J. V.; Foresman, J. B.; Cioslowski, J.; Stefanov, B. B.; Nanayakkara, A.; Challacombe, M.; Peng, C. Y.; Ayala, P. Y.; Chen, W.; Wong, M. W.; Andres, J. L.; Replogle, E. S.; Gomperts, R.; Martin, R. L.; Fox, D. J.; Binkley, J. S.; Defrees, D. J.; Baker, J.; Stewart, J. P.; Head-Gordon, M.; Gonzales, C.; Pople, J. A. *Gaussian 94*, revision E.1; Gaussian, Inc.: Pittsburgh, PA, 1995.

(109) Becke, A. D. *J. Chem. Phys.* **1993**, *98*, 5648−5652.